Automatic Control for Chase Aircraft

Takeshi Yamasaki*, Keisuke Enomoto, Daiki Tanaka, Hiroyuki Takano and Yoriaki Baba
Department of Aerospace Engineering,
National Defense Academy, Kanagawa, Japan

Abstract

Many kinds of unmanned aerial vehicles (UAVs) have been developed for a few decades and some of them are now in operational use. Although each UAV as well as a piloted aircraft might have restrictions to execute some tasks simultaneously or to carry some payloads, one with an automatic chase aircraft might have the potential of multi-capabilities to conduct a variety of missions or to carry more storages. This paper introduces a chase UAV control system to enhance a leader (reference) aircraft capability which has storage restriction. The automatic chase guidance and control system will be introduced with the pure pursuit guidance law combined with relative velocity error corrections, and a dynamic inversion technique in order to generate the guidance forces.

Key Word : UAV, automatic, pure pursuit guidance, dynamic inversion

Nomenclature

x, y, z	:	Components of position vector w.r.t. inertial axes $[m]$
u, v, w	:	Components of airplane velocity along x, y, z body axes $[m/s]$
p, q, r	:	Components of airplane angular velocity about x, y, z body axes $[rad/s]$
ϕ, θ, ψ	:	Euler angles $[rad]$ or $[\mathrm{deg}]$
$\delta_e, \delta_a, \delta_r$	:	deflection of elevator, aileron and rudder $[rad]$ or $[\mathrm{deg}]$
L	:	Lift $[N]$
Y	:	Side force $[N]$
D	:	Drag $[N]$
$F_{\tilde{X}}, F_{\tilde{Y}}, F_{\tilde{Z}}$	:	Guidance forces $[N]$ (wind axes related to inertial axes by flight path angles)
F_X, F_Y, F_Z	:	Guidance forces (Body axes) $[N]$
F_T	:	Thrust $[N]$
$\boldsymbol{F}$	:	Force vector
q_t	:	Dynamic pressure $[N/m^2]$
$g, \boldsymbol{g}$	:	Acceleration due to gravity $[m/s^2]$ and gravity vector
$\boldsymbol{V}$	:	Velocity vector

* Research Associate
E-mail : ymski@nda.ac.jp

V : Airplane resultant velocity $[m/s]$
ρ : Air density $[kg/m^3]$
m : Mass $[kg]$
S : Wing area $[m^2]$
b : Wing span $[m]$
$\bar{c}$: Wing mean aerodynamic chord $[m]$
h : Altitude $[m]$
α : Angle of attack $[rad]$ or $[\mathrm{deg}]$
α_0 : Zero lift angle of attack $[rad]$
γ : Vertical flight path angle $[rad]$ or $[\mathrm{deg}]$
λ : Horizontal flight path angle $[rad]$ or $[\mathrm{deg}]$
N : Navigation constant
$K_\alpha, K_\beta, K_\phi$: Slow mode controller gains
K_p, K_q, K_r : Fast mode controller gains
$\boldsymbol{a}$: Acceleration vector
C_L : Lift coefficient
$C_{L\alpha}$: Lift-curve slope $[/rad]$
C_D : Drag coefficient
C_{D0} : Zero lift drag coefficient
$\boldsymbol{R}$: Line of sight (LOS) vector
R : Relative distance $[m]$
$\boldsymbol{E}$: Rotation transformation matrix
I_X, I_Y, I_Z : Moments of inertia $[kg \cdot m^2]$
$C_{X,t}, C_{Y,t}, C_{Z,t}$: Aerodynamic force coefficients
$C_{l,t}, C_{m,t}, C_{n,t}$: Aerodynamic moment coefficients
$[]_C$: Concerned with the chase aricraft
$[]_{LDR}$: Concerned with the leader aircraft
$[]_d$: Indicate a desired command
$[]_w$: Concerned with the wind axes
$\dot{[\ ]}$: Time derivative

Introduction

Recently, the dramatic development of UAVs can be seen in the world and a huge variety of tasks such as surveillance, reconnaissance, sampling and so on, are being conducted. Although each UAV as well as a piloted aircraft has restrictions on payloads and the scope of the tasks, an additional automatically chasing UAV may be able to compensate those restrictions or expand their ability to carry much payloads and to conduct some tasks simultaneously. We introduce an automatic control system for a chase aircraft. Autonomous formation flight control algorithm was developed using linear equations of motion and PID control [1], or point mass based analysis [2]. Using 6 Degree-of-freedom non-linear equations of motion based control system may provide high-maneuverability to autonomous

chase aircraft for a rigid-body six degree of freedom model. Dynamic inversion techniques [3-5] are one of the most known control schemes on non-linear dynamical systems. A dynamic inversion technique may need guidance forces for its input determination. Proportional navigation [6] may be considered to generate the guidance force, but unlike the case of missiles, the chase aircraft may have almost the same amount of the velocity as a leader aircraft. That means the chase aircraft might fly away from the leader aircraft when the relative velocity is negative [6]. In this reason, the pure pursuit guidance law is applied to generate the guidance forces. The pure pursuit guidance law is to make the chase aircraft heading towards the leader at any time. A velocity control system with the pure pursuit guidance system is necessary for collision avoidance.

In the paper, we will explain rigid-body six degree-of-freedom non-linear equations of motion. Then we will discuss the automatic guidance and control system for chase aircraft, which is based on the pure pursuit guidance law in conjunction with the dynamic inversion technique and velocity control, followed by a several simulation results.

Guidance and Control System

Equations of motion

Figure 1 illustrates the coordinate system employed in this study. The equations of motion for a rigid body airplane with respect to a body-fixed axis system can be expressed as :

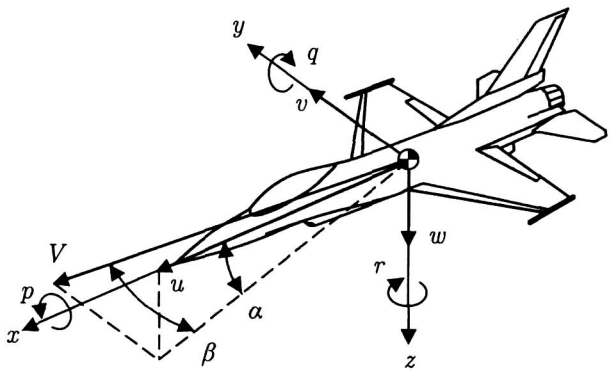

Fig. 1. The coordinate system

$$\dot{x} = u\cos\theta\cos\psi + v(\sin\phi\sin\theta\cos\psi - \cos\phi\sin\psi) + w(\cos\phi\sin\theta\cos\psi + \sin\phi\sin\psi) \tag{1}$$

$$\dot{y} = u\cos\theta\sin\psi + v(\sin\phi\sin\theta\sin\psi + \cos\phi\cos\psi) + w(\cos\phi\sin\theta\sin\psi - \sin\phi\cos\psi) \tag{2}$$

$$\dot{z} = -u\sin\theta + v\sin\phi\cos\theta + w\cos\phi\cos\theta \tag{3}$$

$$\dot{u} = rv - qw - g\sin\theta + \frac{q_t S}{m} C_{X,t} + \frac{F_T}{m} \tag{4}$$

$$\dot{v} = pw - ru + g\cos\theta\sin\phi + \frac{q_t S}{m} C_{Y,t} \tag{5}$$

$$\dot{w} = qu - pv + g\cos\theta\cos\phi + \frac{q_t S}{m} C_{Z,t} \tag{6}$$

$$\dot{\phi} = p + q\sin\phi\tan\theta + r\cos\phi\tan\theta \tag{7}$$

$$\dot{\theta} = q\cos\phi - r\sin\phi \tag{8}$$

$$\dot{\psi} = q\sin\phi\sec\theta + r\cos\phi\sec\theta \tag{9}$$

$$\dot{p} = \frac{I_Y - I_Z}{I_X}qr + \frac{I_{XZ}}{I_X}(\dot{r} + pq) + \frac{q_t Sb}{I_X}C_{l,t} \tag{10}$$

$$\dot{q} = \frac{I_Z - I_X}{I_Y}pr + \frac{I_{XZ}}{I_Y}(r^2 - p^2) + \frac{q_t S\overline{c}}{I_Y}C_{m,t} \tag{11}$$

$$\dot{r} = \frac{I_X - I_Y}{I_Z}pq + \frac{I_{XZ}}{I_Z}(\dot{p} - qr) + \frac{q_t Sb}{I_Z}C_{n,t} \tag{12}$$

where we assumed aerodynamic coefficients as follows:

$$C_{X,t} = C_{X,t}(\alpha, \beta, \frac{\overline{c}q}{2V}, \delta_e) \tag{13}$$

$$C_{Y,t} = C_{Y,t}(\alpha, \beta, \frac{bp}{2V}, \frac{br}{2V}, \delta_a, \delta_r) \tag{14}$$

$$C_{Z,t} = C_{Z,t}(\alpha, \beta, \frac{\overline{c}q}{2V}, \delta_e) \tag{15}$$

$$C_{l,t} = C_{l,t}(\alpha, \beta, \frac{bp}{2V}, \frac{br}{2V}, \delta_a, \delta_r) \tag{16}$$

$$C_{m,t} = C_{m,t}(\alpha, \beta, \frac{\overline{c}q}{2V}, \delta_e) \tag{17}$$

$$C_{n,t} = C_{n,t}(\alpha, \beta, \frac{bp}{2V}, \frac{br}{2V}, \delta_a, \delta_r) \tag{18}$$

The pure pursuit guidance law

Assuming that a chase aircraft pursues a leader (reference) aircraft with the velocity of $\boldsymbol{V}_{C,w}$ as shown in Fig. 2.

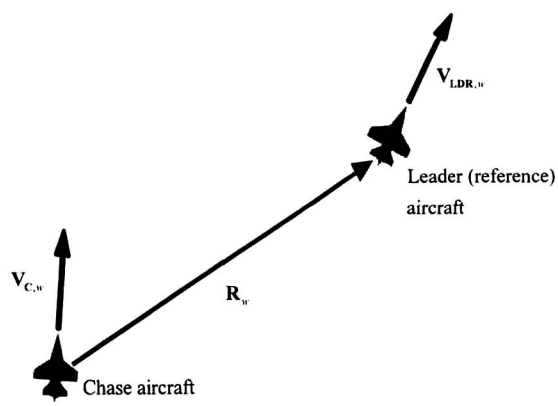

Fig. 2. Position view of the chase and the leader aircraft

The following equation is satisfied if the line of sight (LOS) vector $\boldsymbol{R}_w$ and the chase aircraft's velocity vector $\boldsymbol{V}_{C,w}$ are heading towards the same direction.

$$\boldsymbol{V}_{C,w} \times \boldsymbol{R}_w = \boldsymbol{0} \tag{19}$$

In order to guide the chase aircraft to the pure pursuit course, the following acceleration is needed.

$$\boldsymbol{a}_w = \frac{N(\boldsymbol{V}_{C,w} \times \boldsymbol{R}_w) \times \boldsymbol{V}_{C,w}}{R^2} \tag{20}$$

From the Newton's second law, the required guidance force with the gravity compensation can be expressed as:

$$\boldsymbol{F}_w = m(\boldsymbol{a}_w - \boldsymbol{g}_w) \tag{21}$$

Derivation of command values

The guidance force appeared in Equation (21) is transformed from wind axes into body axes, that is

$$\begin{pmatrix} F_X \\ F_Y \\ F_Z \end{pmatrix} = E(\phi,\theta,\psi) \cdot E^{-1}(0,\gamma,\lambda) \begin{pmatrix} F_{\hat{X}} \\ F_{\hat{Y}} \\ F_{\hat{Z}} \end{pmatrix} \tag{22}$$

Using the guidance force in Eq. (22) desired angle of attack, sideslip angle and bank angle can be expressed as follows:

$$\alpha_d = \frac{1}{C_{L\alpha}} \left(\frac{L_d - F_T \sin\alpha}{q_t S} \right) + \alpha_0 \tag{23}$$

$$\beta_d = 0 \tag{24}$$

$$\phi_d = \phi + \Delta\phi_d \tag{25}$$

where

$$L_d = \sqrt{F_{\hat{Y}}^2 + F_{\hat{Z}}^2} \tag{26}$$

$$\Delta\phi_d = \tan^{-1} \frac{F_Y}{-F_Z} \tag{27}$$

Dynamic inversion

After some processes with Eqs. (4)−(6) and (7), slow mode equations of motion concerned with α, β and ϕ can be derived as:

$$\dot{\alpha} = \{ -L - F_T \sin\alpha + mg(\cos\phi\cos\theta\cos\alpha + \sin\theta\sin\alpha) \} / (mV\cos\beta) + q - \tan\beta(p\cos\alpha + r\sin\alpha) \tag{28}$$

$$\dot{\beta} = \{ Y - F_T \cos\alpha\sin\beta + mg(\sin\theta\cos\alpha\sin\beta + \sin\phi\cos\theta\cos\beta - \cos\phi\cos\theta\sin\alpha\sin\beta) \} / (mV) + p\sin\alpha - r\cos\alpha \tag{29}$$

$$\dot{\phi} = p + q\sin\phi\tan\theta + r\cos\phi\tan\theta \tag{30}$$

Solving Eqs. (28)−(30) for $(p, q, r)^T$ and replacing respective $(p, q, r)^T$ and $(\dot{\alpha}, \dot{\beta}, \dot{\phi})^T$ to desired $(p_d, q_d, r_d)^T$ and $(U_\alpha, U_\beta, U_\phi)^T$, one obtains

$$\begin{pmatrix} p_d \\ q_d \\ r_d \end{pmatrix} = \begin{pmatrix} -\cos\alpha\tan\beta & 1 & -\sin\alpha\tan\beta \\ \sin\alpha & 0 & -\cos\alpha \\ 1 & \sin\phi\tan\theta & \cos\phi\tan\theta \end{pmatrix}^{-1} \begin{pmatrix} U_\alpha - A_\alpha \\ U_\beta - A_\beta \\ U_\phi \end{pmatrix} \tag{31}$$

where

$$\begin{pmatrix} U_\alpha \\ U_\beta \\ U_\phi \end{pmatrix} = \begin{pmatrix} K_\alpha(\alpha_d - \alpha) \\ K_\beta(\beta_d - \beta) \\ K_\phi(\phi_d - \phi) \end{pmatrix} \tag{32}$$

$$A_\alpha = \{ -L - F_T \sin\alpha + mg(\cos\phi\cos\theta\cos\alpha + \sin\theta\sin\alpha) \} / mV\cos\beta \tag{33}$$

$$A_\beta = \{ Y - F_T \cos\alpha\sin\beta + mg(\sin\theta\cos\alpha\sin\beta + \sin\phi\cos\theta\cos\beta - \cos\phi\cos\theta\sin\alpha\sin\beta) \} / mV \tag{34}$$

$(U_\alpha, U_\beta, U_\phi)^T$ may be designed to satisfy a required performance. The proportional control is employed in this study for simplicity.

Eq. (31) indicates the inverse system of the slow mode equations.

The matrix form of Eqs. (10)−(12) can be expressed as:

$$\begin{pmatrix} \dot{p} \\ \dot{q} \\ \dot{r} \end{pmatrix} = \begin{pmatrix} A_p \\ A_q \\ A_r \end{pmatrix} + \begin{pmatrix} B_{pa} & 0 & B_{pr} \\ 0 & B_{qe} & 0 \\ B_{ra} & 0 & B_{rr} \end{pmatrix} \begin{pmatrix} \delta_a \\ \delta_e \\ \delta_r \end{pmatrix} \tag{35}$$

where

$$A_p = \{ I_{XZ}(I_X - I_Y + I_Z)pq + (-I_Z^2 + I_Y I_Z - I_{XZ}^2)qr + I_Z q_t Sb[C_{l\beta}\beta + \frac{b}{2V}(C_{lp}p + C_{lr}r)] + I_{XZ} q_t Sb[C_{n\beta}\beta + \frac{b}{2V}(C_{np}p + C_{nr}r)] \} / (I_X I_Z - I_{XZ}^2) \tag{36}$$

$$A_q = \{ (I_Z - I_X)pr + I_{XZ}(r^2 - p^2) + q_t S\bar{c}(C_{m0} + C_{m\alpha}\alpha + \frac{\bar{c}}{2V} C_{mq} q) \} / I_Y \tag{37}$$

$$A_r = \{ (I_{XZ}^2 - I_X I_Y + I_X^2)pq - I_{XZ}(I_X - I_Y + I_Z)qr + I_{XZ} q_t Sb[C_{l\beta}\beta + \frac{b}{2V}(C_{lp}p + C_{lr}r)] + I_X q_t Sb[C_{n\beta}\beta + \frac{b}{2V}(C_{np}p + C_{nr}r)] \} / (I_X I_Z - I_{XZ}^2) \tag{38}$$

$$B_{pa} = q_t Sb(I_Z C_{l\delta_a} + I_{XZ} C_{n\delta_a}) / (I_X I_Z - I_{XZ}^2) \tag{39}$$

$$B_{pr} = q_t Sb(I_Z C_{l\delta_r} + I_{XZ} C_{n\delta_r}) / (I_X I_Z - I_{XZ}^2) \tag{40}$$

$$B_{qe} = q_t S\bar{c} C_{m\delta_e} / I_Y \tag{41}$$

$$B_{ra} = q_t Sb(I_{XZ} C_{l\delta_a} + I_X C_{n\delta_a}) / (I_X I_Z - I_{XZ}^2) \tag{42}$$

$$B_{rr} = q_t Sb(I_{XZ} C_{l\delta_r} + I_X C_{n\delta_r}) / (I_X I_Z - I_{XZ}^2) \tag{43}$$

Solving Eq. (35) for $(\delta_e, \delta_a, \delta_r)$ and replacing respective $(\delta_e, \delta_a, \delta_r)^T$ and $(\dot{p}, \dot{q}, \dot{r})^T$ to desired $(\delta_{e,d}, \delta_{a,d}, \delta_{r,d})^T$ and $(U_p, U_q, U_r)^T$ yield

$$\begin{pmatrix} \delta_{a,d} \\ \delta_{e,d} \\ \delta_{r,d} \end{pmatrix} = \begin{pmatrix} B_{pa} & 0 & B_{pr} \\ 0 & B_{qe} & 0 \\ B_{ra} & 0 & B_{rr} \end{pmatrix}^{-1} \begin{pmatrix} U_p - A_p \\ U_q - A_q \\ U_r - A_r \end{pmatrix} \tag{44}$$

where

$$\begin{pmatrix} U_p \\ U_q \\ U_r \end{pmatrix} = \begin{pmatrix} K_p(p_d - p) \\ K_q(q_d - d) \\ K_r(r_d - d) \end{pmatrix} \tag{45}$$

The proportional control is also applied for the fast mode control.

Acceleration and deceleration of the chase aircraft

The chase aircraft velocity should be controlled the same velocity as the leader aircraft in order to avoid the collision when the chase aircraft come close to the leader. A thrust command for deceleration / acceleration is calculated from the following equation.

$$F_{T_C} = F_X + \frac{m\frac{V_{LDR}^2 - V_C^2}{2R} + D + F_Z \sin\alpha}{\cos\alpha} \tag{46}$$

The first tem in the numerator of the second term in Eq. (46) indicates that thrust input is decreased (or increased) to decelerate (or accelerate) the chase aircraft to the target velocity during the R −distance flight.

A thrust command for further acceleration or deceleration may be given by

$$F_{T_C} = F_X + \frac{m\frac{(V_{LDR} + \Delta V)^2 - V_C^2}{2R} + D + F_Z \sin\alpha}{\cos\alpha} \tag{47}$$

The difference between Eq. (46) and Eq. (47) is that V_{LDR} is set $V_{LDR} + \Delta V$ in Eq. (47) Using this command, the chase aircraft can reduce the distance from the leader if $\Delta V > 0$.

Simulations

The YF−16 model [7] is used in our simulations to demonstrate the chase aircraft guidance and control system. Two simulation results are depicted in this paper. One is a rectilinear flight chasing result and the other is a level turn case. Table 1 gives the initial settings of these simulations. The both simulations start the same conditions. The chase aircraft position far away from the leader aircraft at the beginning. ΔV in Equation (47) is set $0.2 \times 10^{-3} R\ V_{LDR}$ when $R > 10[m]$, otherwise ΔV is set zero in order to avoid the collision. We set the following assumption to simplify the problem and to demonstrate the total system

a. Ambient atmosphere is stationary.
b. The mass of the aircraft is constant and the engine momentum is negligible.
c. The aircraft model is available and aerodynamic uncertainties are negligible.
d. The leader aircraft's direction, distance and relative velocity information is available.

Table 1. Simulation settings

	Initial values					
	The chase aircraft			The leader aircraft		
Case1: Rectilinear level flight	x :	0	[m]	x_{LDR} :	1000	[m]
	y :	0	[m]	y_{LDR} :	100	[m]
	h :	600	[m]	h_{LDR} :	700	[m]
	V :	180	[m/s]	V_{LDR} :	205	[m/s]
Case2: Level turn	α :	2.0	[deg]	α_{LDR} :	1.8	[deg]
	β :	0.0	[deg]	β_{LDR} :	0.0	[deg]
	γ :	0.0	[deg]	γ_{LDR} :	0.0	[deg]
	ϕ :	0.0	[deg]	ϕ_{LDR} :	0.0	[deg]
	T :	8000	[N]	T_{LDR} :	8000	[N]

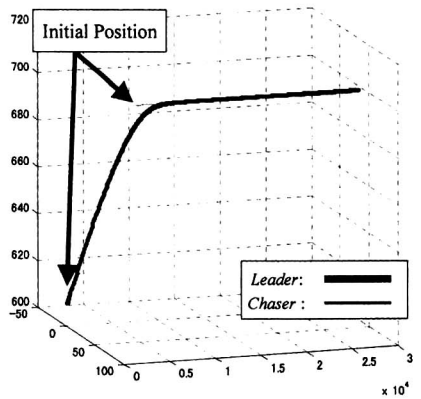

Fig. 3. The trajectories of the leader and the chase aircraft. (Rectilinear level flight)

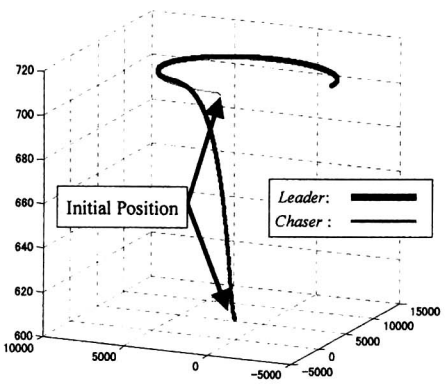

Fig. 4. The trajectories of the leader and the chase aircraft. (Level turn)

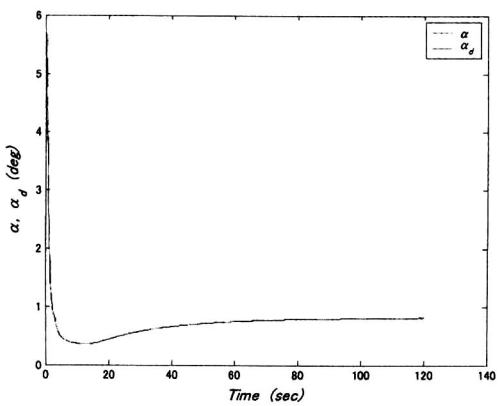

Fig. 5. The time histories of the desired and the real angle of attack of the chase aircraft. (Rectilinear level flight)

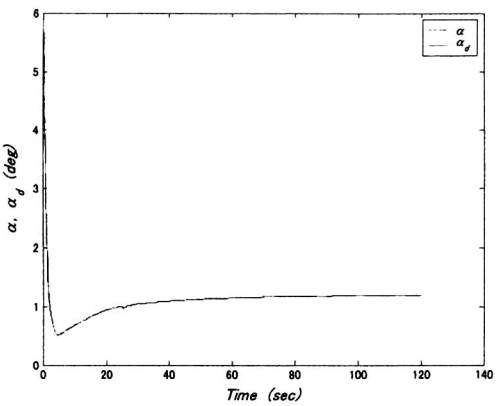

Fig. 6. The time histories of the desired and the real angle of attack of the chase aircraft. (Level turn)

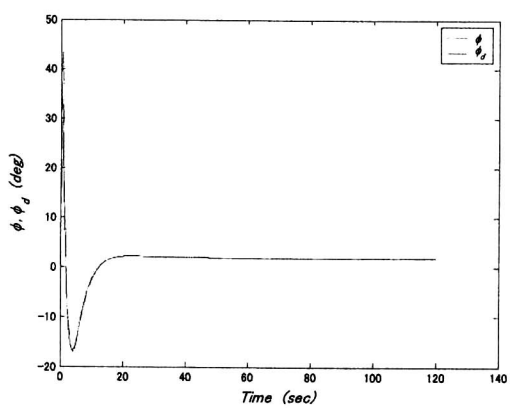

Fig. 7. The time histories of the desired and the real bank angle of the chase aircraft. (Rectilinear level flight)

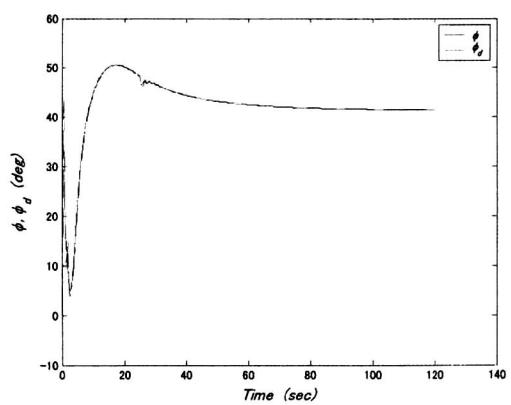

Fig. 8. The time histories of the desired and the real bank angle of the chase aircraft. (Level turn)

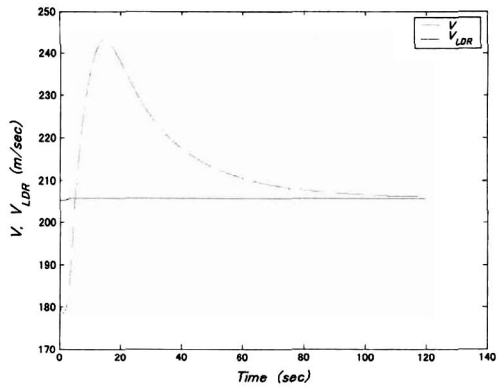

Fig. 9. The time histories of velocities of the leader and the chase aircraft. (Rectilinear level flight)

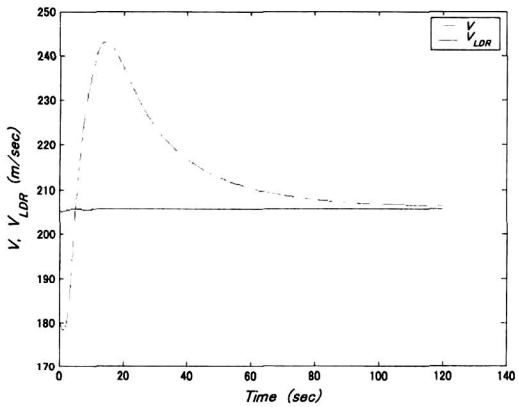

Fig. 10. The time histories of velocities of the leader and the chase aircraft. (Level turn)

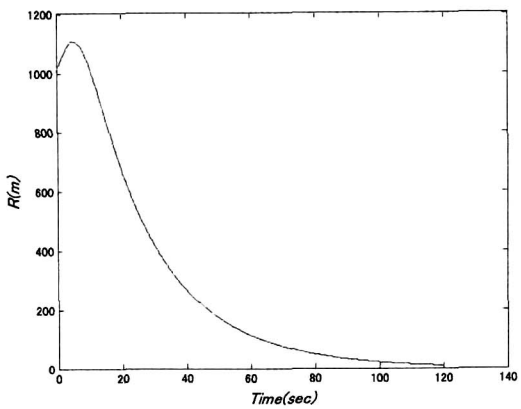

Fig. 11. The time history of the relative distance. (Rectilinear level flight)

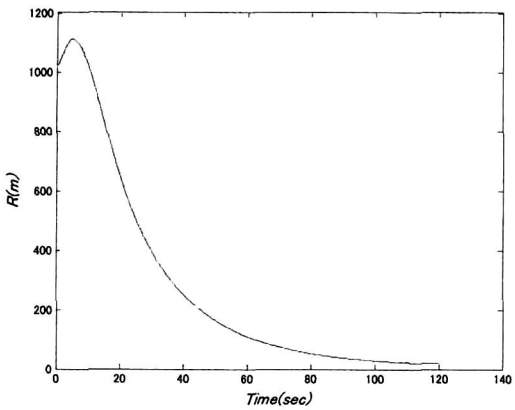

Fig. 12. The time history of the relative distance.(Level turn)

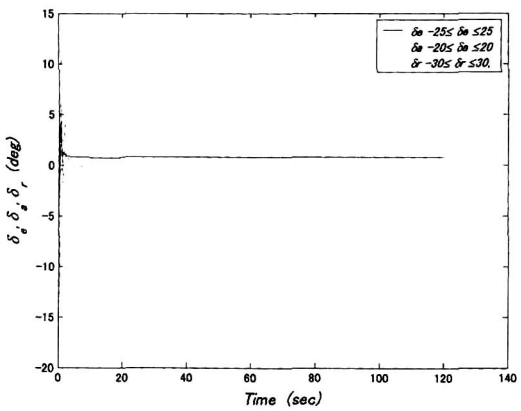

Fig. 13. The time history of the control surfaces angle. (Rectilinear level flight)

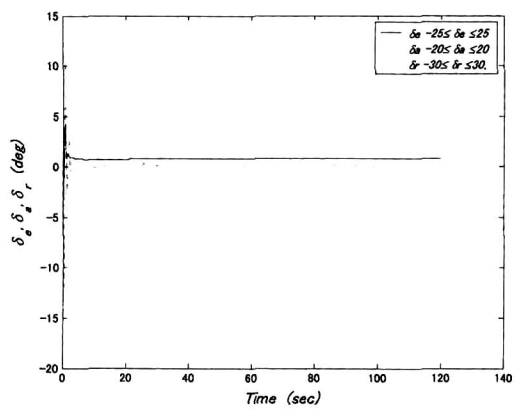

Fig. 14. The time history of the control surfaces angle. (Level turn)

The assumption a and c may be violated in most cases, but robustness for model uncertainties and external disturbance such as gust may be compensated with the inner loop design of the dynamic inversion controller appeared in references 8 and 9 (for example) instead of using the proportional control in Eq. (45).

Numerical simulation results are shown in Figures 3 and 4. Figs. 3 and 4 show the trajectories of the leader and the chase aircraft. Fig. 3 gives a rectilinear flight while Fig. 4 indicates level turn. The thick lines indicate the leader trajectories and the thin ones are concerned with the chase aircraft. Figs. 3-6 show how well the chase aircraft pursues the leader aircraft. Figs. 5-6 and Figs. 7-8 are the time histories of α and α_d, ϕ and ϕ_d in each maneuver, respectively. As shown in Figs. 5-8, the desired angle of attack and bank angle are well tracked by the real ones. Figs. 9-10 are the time histories of the leader and the chase aircraft's velocity in each maneuver. Figs. 9 and 10 show that the chase aircraft velocity gives a good match with the leader's velocity after the initial phase which are different each other due to the effort to catch up. Figs. 11 and 12 show the time history of the relative distance. The initial negative relative velocity to the leader causes the chase aircraft to go farther away from the leader in the beginning. The chase aircraft shortened the distance to the leader aircraft, gradually. In Figs. 13 and 14, the control surfaces are always actuated under the limitations.

Conclusions

An automatic chase aircraft guidance and control system is introduced. The system is proved to work well in chasing the leader aircraft. Although an optimal navigation constant and dynamic control gains may depend on the situation or aircraft performance, the pure pursuit guidance law is useful to generate the guidance force and the dynamic inversion technique gives high maneuverable chasing capability to an autonomous chase aircraft.

References

1. H. Akiyama, T. Harada, I. Sudo, A. Yokoyama, K. Masui and H. Tomita, "Flight Demonstration for Autonomous Formation Flight Control Algorithm", *Proceeding of the 43rd JSASS Aircraft symposium*, pp. 472-476, 2005.

2. M-J Tahk, C-S Park and C-K Ryoo, "Line of Sight Guidance Laws for Formation Flight," *Journal of Guidance, Control, and Dynamics*, Vol. 28, No. 4, pp.708-716, AIAA, 2005.

3. R. W. Brockett., "Feedback Invariants for Nonlinear Systems", *Proceeding of the 1978 IFAC World Congress*, pp. 1115-1120, 1978.

4. S. H. Lane and R. F. Stengel, "Flight Control Design Using Non-linear Inverse Dynamics", *Automatica*, Vol. 24, pp. 471-483, 1988.

5. S. Ochi, H. Takano and Y. Baba, "Flight Trajectory Tracking System applied to inverse control for aerobatic maneuvers", *Inverse Problems in Engineering Mechanics III*, Elsevier Science Ltd., pp. 337-344, 2002.

6. P. Zarchan,: *Tactical and Strategic Missile Guidance -Fourth Edition-*, Progress in Astronautics and Aeronautic, Vol. 176, AIAA, 2002.

7. W. P. Gilbert, L. T. Nguyen and R. W. Van Gunst, "Simulator Study of the Effectiveness of an Automatic Control System Designed to Improve the High-Angle-of-Attack Characteristics of a Fighter Airplane", NASA, TN D-8176, 1976.

8. D. P. Boyle and G. E. Chamitoff, "Autonomous Maneuver Tracking for Self-Piloted Vehicles", *Journal of Guidance, Control and Dynamics*, Vol. 22, No. 1, pp. 58-67, 1999.

9. D. Higashi, Y. Shimada, K. Uchiyama, S. Ishimoto and Y. Minami, "Design of Nonparametric Adaptive Flight Controller for Automatic Landing Using Dynamic Inversion and Disturbance-Accommodation-Control Observer", *Proceeding of 2006 KSAS-JSAS Joint International Symposium*, pp. 227-233, 2006.